International Journal of Mechanical, Industrial and Aerospace Sciences
ISSN: 2517-9950
Vol:3, No:8, 2009

Fatigue Crack Growth Behavior in Dissimilar Metal Weldment of Stainless Steel and Carbon Steel

K. Krishnaprasad, and Raghu V. Prakash

***Abstract*—**Constant amplitude fatigue crack growth (FCG) tests were performed on dissimilar metal welded plates of Type 316L Stainless Steel (SS) and IS 2062 Grade A Carbon steel (CS). The plates were welded by TIG welding using SS E309 as electrode. FCG tests were carried on the Side Edge Notch Tension (SENT) specimens of 5 mm thickness, with crack initiator (notch) at base metal region (BM), weld metal region (WM) and heat affected zones (HAZ). The tests were performed at a test frequency of 10 Hz and at load ratios (R) of 0.1 & 0.6. FCG rate was found to increase with stress ratio for weld metals and base metals, where as in case of HAZ, FCG rates were almost equal at high ΔK. FCG rate of HAZ of stainless steel was found to be lowest at low and high ΔK. At intermediate ΔK, WM showed the lowest FCG rate. CS showed higher crack growth rate at all ΔK. However, the scatter band of data was found to be narrow. Fracture toughness (Kc) was found to vary in different locations of weldments. Kc was found lowest for the weldment and highest for HAZ of stainless steel. A novel method of characterizing the FCG behavior using an Infrared thermography (IRT) camera was attempted. By monitoring the temperature rise at the fast moving crack tip region, the amount of plastic deformation was estimated.

***Keywords*—**Dissimilar metal weld, Fatigue Crack Growth, fracture toughness, Infrared thermography.

I. Introduction

IN power plants, stainless steel (SS) is often used for high temperature structural components, in view of the good high temperature mechanical properties. Carbon steel (CS) is chosen for components subject to lower temperature. There are bimetallic welded joints at interfaces between stainless steel and carbon steel. Dissimilar metal weldments present difficulties because of macro and micro discontinuities, residual stresses and possible misalignment, which makes it the prime location of fatigue failures. The residual tensile stresses in the weld region may reach values equal to the yield strength and can contribute to the lower fatigue resistance of weldments. Basically there are three weldment regions, viz., Parent or Base metal (BM), Deposited weld metal (WM) and Heat Affected Zone (HAZ). These three regions can have different microstructures, residual stresses, discontinuities, monotonic strength, ductility and fracture toughness properties. HAZ, which is subjected to higher temperature, may or may not cause re-crystallization and hence the mechanical properties and metallurgical structures may be similar to or different from that of base metal. [1], [2], [3] have studied FCG behaviors of base metal, weld metal and heat affected zone of various metals using Paris law. They observed an increase in FCG rate from weld metal towards base metal, although the variation is very less. Enhanced FCG resistance of weld is due to presence of acicular ferrite in the structure. [4] conducted fracture tests on weldments of 1Cr-1Mo-0.25 V steel containing a definite HAZ region, using under-matched and over-matched weld metals. They found that the crack trajectories are largely influenced by the strength mismatch (over matched / under matched). [5] have carried out experimental and numerical investigations of crack trajectories of bronze–steel weldment and found that the crack proceeded in the direction of the weaker material.

For damage tolerant design and integrity assessment of these components, knowledge on fatigue crack growth properties of the various regions of dissimilar metal weldments are essential. This study is aimed at characterizing the fatigue crack growth (FCG) properties of various regions of weldment using constant amplitude FCG rate tests performed as per ASTM 647.

A novel method of characterization of FCG rates of this weldment is attempted by using an Infra Red Thermography (IRT) technique. IRT is based on the principle of surface temperature variation occurring in a material due to elastic and plastic deformations. During elastic deformation under tensile load, there will be an increase in the volume of specimen resulting a decrease in surface temperature, while compressive load results in a decrease in volume, hence an increase in temperature. But beyond the yield point, a sudden reversal in the direction of temperature change occurs as thermal energy is released due to occurrence of irreversible plastic deformation. The radiation energy emitting from materials due to these temperature change is in the infra red range and can be recorded by an Infra Red Thermography (IRT) camera, which represents this variation in the form of thermal image. Thus, IRT can be used as a non destructive, non-contact and real-time technique and as a NDE tool. From the thermal images of a propagating crack tip under fatigue loading, amount of plastic deformation can be found out. [6], [7] and [8] used the temperature data at the tip of propagating crack to calculate the fracture toughness under static and dynamic (fatigue) load. [9] indicated that the fracture toughness value

K. Krishnaprasad is currently with Department of Mechanical Engineering, Indian Institute of Technology Madras, Chennai 600 036, India, on deputation from Indira Gandhi Centre of Atomic Research, Kalpakkam, India (e-mail: kkprasad@igcar.gov.in).

Raghu V. Prakash is with the Department of Mechanical Engineering, Indian Institute of Technology Madras, Chennai 600 036, India (phone: +91-44-2257 4694; e-mail: raghuprakash@iitm.ac.in).

can be estimated by finding out the temperature change at the onset of stable crack propagation.

In the present work, temperature response of crack tip during the FCG is studied. An attempt is made to correlate the temperature data obtained during the FCG of various locations in weldment with the fracture toughness values found out from constant amplitude FCG tests.

II. Experimental Procedure

A. Constant Amplitude FCG Test

Dissimilar metal weld specimen was prepared by TIG welding of Type 316L steel plate of 5 mm thickness to IS 2062 Grade-A carbon steel plate of same thickness. The weld was single V groove butt weld and hence the edge preparation was done prior to welding. Electrode conforming to specification of E 309 was used during welding. Single Edge Notch tension (SENT) specimens of 25x100x5 mm were prepared with an U-notch of 0.1 mm radius and 3mm deep cut at various locations of weldments by wire cutting. The FCG tested specimens are shown in Fig. 1. Material composition of base metals (SS & CS) and weld metal (WM) are listed in Table I.

Fig. 1 FCG tested welded specimens

TABLE I
Chemical Composition of Base Metals and Weld Metal

Type 316L Stainless Steel (Base Metal)									
Element	C	Mn	Si	P	S	Cr	Mo	Ni	N
Wt % (max)	0.03	2.0	0.75	0.045	0.03	18.0	3.0	14.0	0.1
IS 2062 Grade A Carbon Steel (Base Metal)									
Element	C	Mn	Si	P	S	C.E			
Wt % (max)	0.23	1.5	0.4	0.05	0.05	0.42			
Weld Metal (E309)									
Element	C	Mn	Si	Cr	Ni				
Wt % (max)	0.15	2.5	0.9	26	15				

The experiments were carried out in a 100 kN MTS servo hydraulic system, shown in Fig. 2. The experiments were carried out under tension – tension loading conditions in load control mode. The crack growth was measured with help of a traveling microscope and the corresponding number of cycles was noted from the machine control software to find out the crack growth rate (da/dN). The tests were performed conforming to ASTM E647.

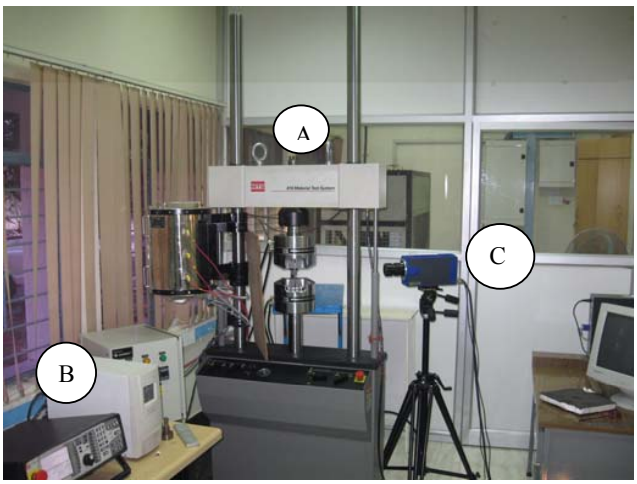

Fig. 2 Experimental set up (A) MTS servo hydraulic system (B) Controller for MTS system (C) Infra red thermography camera

B. Infrared Thermography Measurement

Thermographic measurements were made using a CEDIP Jade LWIR camera (shown in Fig. 2) while the fatigue crack growth rate was in progress on the MTS machine. The IR themography system consists of an infrared camera cooled by electronic control of Stirring cooler. It contains an Hg-Cd-Te detector which is sensitive to infrared radiation in the wavelength range 8-10μm. The main features of the camera are: window size varying from 320x240 to 320x 1 pixel, variation of the frame rate from 5 to 1500 Hz, adjustable integration time from 60 to 500 μs and real-time lock-in detection. This has a 25mm-objective lens, with a focal length of 25 mm and giving a field view of 22°x 16°. The Noise Equivalent Temperature difference (NETD) is 0.02°C at 25°C. The specimen was mounted on the MTS machine and the camera was set on the tripod at least 1 m away from the specimen. The frame rate of camera shall be set at ten times the loading frequency to obtain accurate results. Since the test frequency was 10 Hz, the frame rate was set at 100 frames per second. The image window size was adjusted for clear image viewing of area of interest. A two-point Non Uniformity Correction (NUC) was done by keeping blackbodies maintained at cold and hot temperature in front of the camera. Calibration of camera was done in order to convert the digital data captured by the IR camera into temperature data. This is done on the assumption that the specimen is a black body with a unit emissivity. The specimen was coated with black board

paint, in order to reduce the reflectivity. The specimen held between the hydraulic grippers of MTS system as shown in Fig. 3. The fluctuation in room temperature is taken into account by recording the temperature data of an unloaded specimen kept nearby the test specimen (Fig. 3). The temperature data is store in Automatic Gain Control mode in computer and the data at the region of interest can be extracted in the form of timing graph using Altair software.

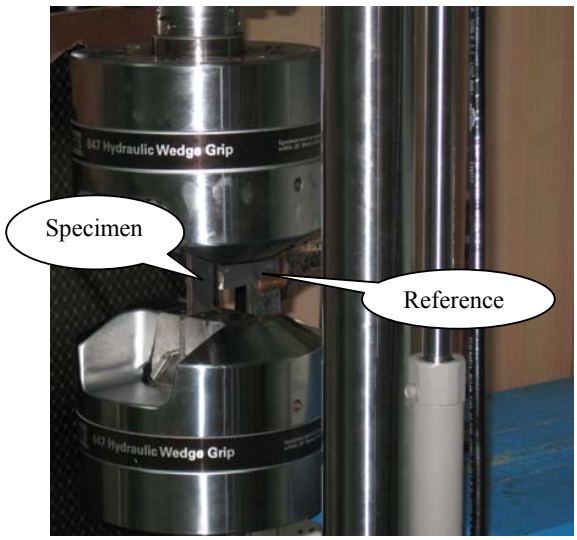

Fig. 3 Specimen mounting details for IRT test

III. Results and Discussions

A. Influence of Load Ratio of FCG Behavior

Crack length (a) Vs Number of cycles (N) plots for various regions of weldment for load ratios, R = 0.1 & 0.6 were plotted. A typical a Vs N plot for stainless steel (base metal) is shown in Fig. 4. It may be noted that the number of cycles required for a particular crack growth is more for R = 0.6. The same trend was followed for all the five regions of weldment. This is due to the low stress amplitude for R = 0.6. The critical crack length to width ratio (a/W) was found out for all regions of weldment. This gives the information about the maximum crack length the material can withstand before catastrophic failure. This was found to be 0.7 for R=0.1 and 0.5 for R=0.6 for all regions of weldment.

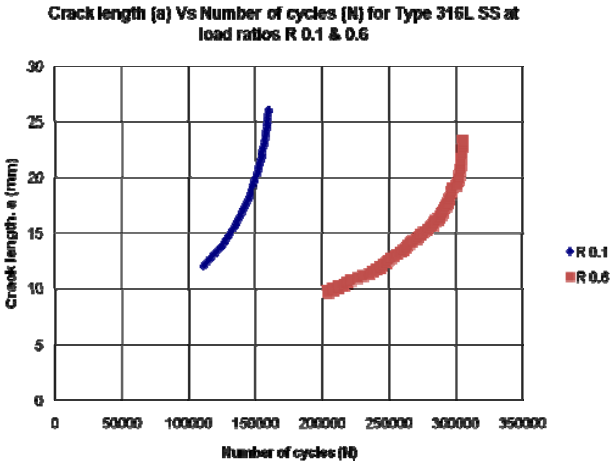

Fig. 4 a Vs N plot for R = 0.1 & 0.6 for Type 316L SS

FCG behavior of base metals, weld metals and HAZ followed the Paris – Erdogan law of the form:

$$\frac{da}{dN} = C(\Delta K)^m \quad (1)$$

It is noted that FCG rate $\left(\frac{da}{dN}\right)$ is found out from the slope of crack length (a) Vs No. of cylces (N) curve. Double logarithmic plots of FCG rate Vs Stress Intensity Factor (ΔK) for various regions of weldments at load ratios of R = 0.1 & 0.6 is shown in Fig. 5.

FCG rate increases with stress ratio for parent metals and weld metal. This is in consistent with observations made by M. P. Mishra et al. for type 316LN stainless steel. [6]. In case of HAZ of SS and CS, it is observed that FCG curve at R = 0.6 overlaps with that of R=0.1 at higher ΔK. This shows that at higher ΔK, the HAZ exhibit crack closure behavior even at load ratio of 0.6. This tendency may be due to the crystallographic change that has taken place either due to over heat during welding or high diffusivity of weld metal into base metal. Fracture toughness values (K_c) was found out from the ΔK value corresponding to the point of fast fracture. K_c values of all five regions of weldment at load ratio, R = 0.1 is given in Table II.

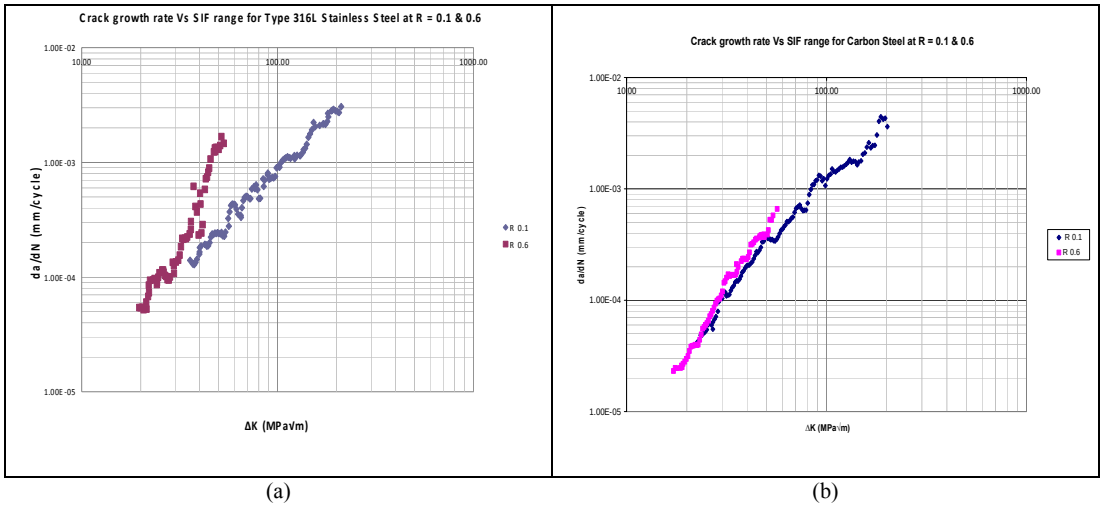

(a) (b)

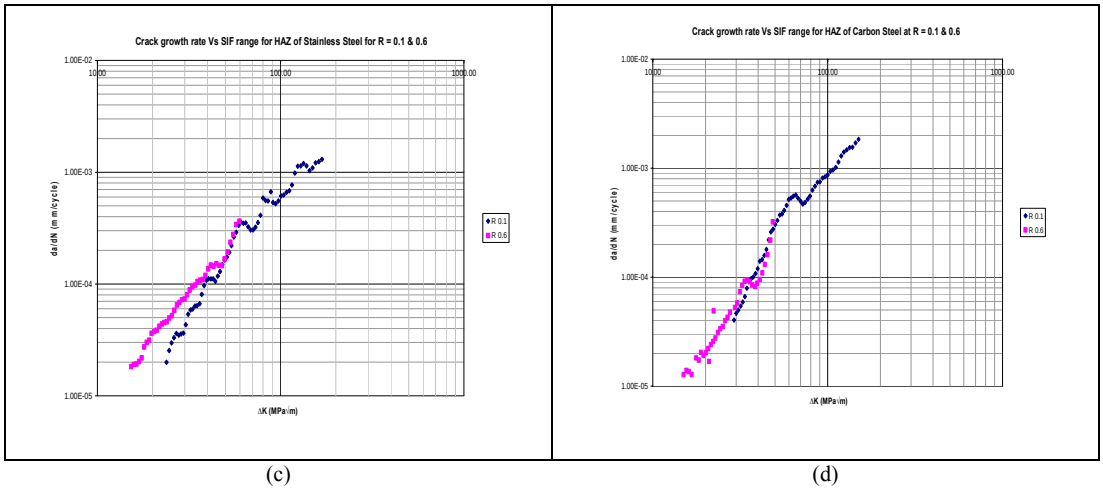

(c) (d)

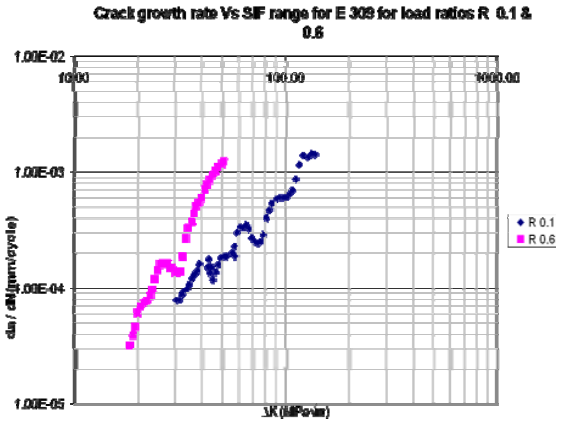

(e)

Fig. 5 Crack propagation rates of base metals, weld metals and HAZ for R = 0.1 & 0.6. (a) Stainless steel base metal, (B) Carbon steel base metal, (c) HAZ of Stainless steel, (d) HAZ of Carbon Steel (e) Weld metal

TABLE II
FRACTURE TOUGHNESS OF VARIOUS REGIONS OF WELDMENT

Region	SS	HAZ of SS	CS	HAZ of CS	Weld metal
K_c (MPa√m)	234.6	186.8	198.5	166.7	152.3

B. FCG Rate at Various Regions of Weldments

da/dN Vs ΔK plots for different various locations in the weldment is shown in Fig. 6. It is found that the difference in the crack growth rates for parent metals, HAZ and weldmetal are small. At higher and lower ΔK ranges, HAZ of SS shows the lowest crack growth rate, where as at the intermediate ΔK ranges, weld metal exhibited the least FCG rate. At higher ΔK, FCG rates of weld metal and base metals converge due to the reduced level of crack closure. FCG rate of CS base metal was found to be highest at all ΔK. The Paris law constant C and m for equation for various locations in weldment are given in Table III. The data in Table II and III shows that fracture toughness of HAZ of SS & CS are lesser than that of their corresponding parent metals, where as the K_{th} is higher for the HAZ. Hence the damage tolerance capability at the HAZ is lower than that of their corresponding base metals.

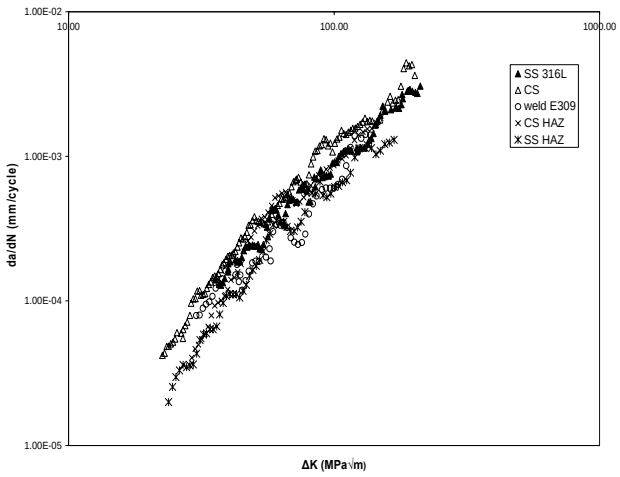

Fig. 6 da/dN Vs ΔK plots of welded specimens with cracks at various locations

TABLE III
PARIS LAW CONSTANTS FOR VARIOUS LOCATIONS IN WELDMENT

Crack location in weldment	C (m/cycle)	m
Stainless steel	2.43E-10	1.77
Carbon Steel	1.13E-10	2.00
HAZ of SS	3.85E-11	2.11
HAZ of CS	4.17E-11	2.18
Weld metal E309	1.52E-10	1.82

The results obtained from IRT technique study on FCG on the weldment is discussed in the following paragraphs.

IV. INFRARED THERMOGRAPHY

A. Temperature Response at Crack Tip

Constant amplitude fatigue loading is applied to specimens, with pre-cracking at various locations in weldment, using MTS system. This is monitored by an IRT camera. Typical temperature response Vs No. of loading cycle plot of a point at a distance "d" on the path of moving crack, perpendicular to the direction of loading in HAZ of CS is shown in Fig. 7.

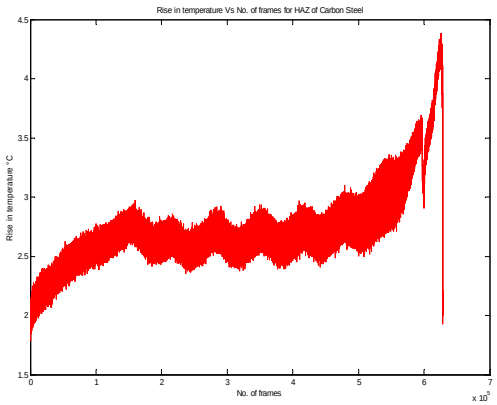

Fig. 7 The typical temperature response Vs No. of cycles plot for a specimen with initial crack at HAZ of CS

Three stages of temperature profile are obtained, viz., an initial increase of average specimen temperature due to increase in plastic strain, a steady state temperature region due to saturation of plastic strain and the specimen attaining thermal equilibrium with environment and finally an abrupt increase in temperature due to high generation caused by damage accumulation. After this, an abrupt rise in temperature is observed at the onset of unstable crack growth as the damage gets accumulated and heat generation is very high. This is followed by a drop in temperature just after the specimen failure. These observations are inline with the experiment carried out by Yang on fatigue test in RPV steels [10]. The temperature response curves for base metals, weld metal and HAZ of weldment at a point in the crack path just before failure of specimen is shown in Fig. 8. The slopes of curves in initial and steady state regions are given in Table IV.

TABLE IV
SLOPES OF TEMPERATURE RESPONSE CURVE

Location of crack	Slope at Initial region	Slope at steady state region
Stainless steel	3E-4	2.5E-7
HAZ of SS	1.3E-5	2.3E-6
Carbon steel	1.7E-5	1.6E-6
HAZ of CS	7.1E-6	5.8E-7
Weld metal	1.1E-5	1.6E-7

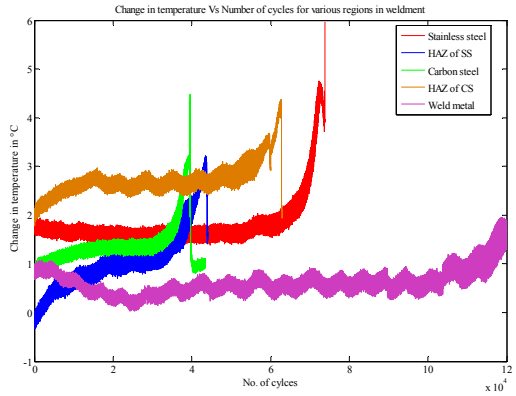

Fig. 8 Temperature response curves for various regions of weldment at points just before the onset of unstable crack propagation

B. *Fracture Toughness Measurement by IRT Technique*

The temperature at a point on the specimen increases as the crack tip approaches it, reaches a maximum instantaneously and then falls immediately after the crack tip passes the point. Since the plastic deformation energy is converted to heat, the change in surface temperature measurement at the crack tip corresponds to the amount of plastic deformation, hence can be correlated to the fracture toughness of the material. [7] and [9] have estimated the fracture toughness following similar method. Maximum change in temperature (ΔT_{max}) at the crack tip at various locations of weldment is given in Table V.

TABLE V
MAXIMUM TEMPERATURE CHANGE AT CRACK TIP

S. No.	Location in weldment	Max. rise in temperature (ΔT_{max}) in °C
1	Weld metal	1.93
2	HAZ of Stainless steel	3.2
3	Carbon steel	3.3
4	HAZ of carbon steel	3.64
5	Stainless steel	4.73

Fig. 9 shows the comparison of Fracture toughness values obtained by FCG tests and the rise in temperature data at the crack tip from IRT for various regions of the weldment.

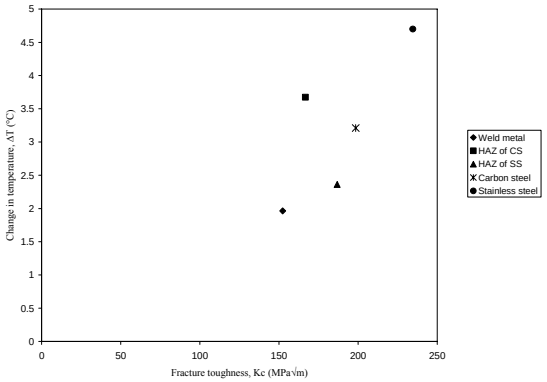

Fig. 9 Correlation between temperature change and fracture toughness in various locations of weldment

The rise in the surface temperature of the specimens correlates well with the fracture toughness values except for HAZ of CS. This may be due to the non uniformity of the crystal structure within the HAZ and due to non uniform heat or due to diffusion. Hence the surface temperature data from IRT can be used in determining the fracture toughness of material.

Fig. 10 shows the temperature response of moving crack tip through out the FCG test up to failure. The slope of the steady stage of this temperature response curve corresponds to the change in ΔK with the number of cycles. The steep rise in temperature at the end of test corresponds to the unstable crack propagation and the maximum temperature shows the accumulated damage at the failure point of specimen.

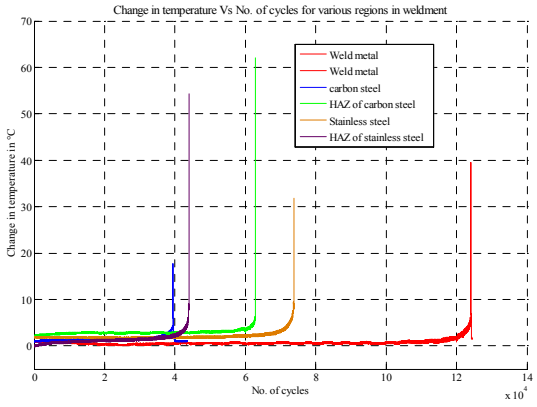

Fig. 10 Temperature response for FCG test on specimens with cracks at various regions of weldment

C. *Determination of Plastic Zone Size by IRT Technique*

When a material is subjected to tensile loading in the elastic limit under adiabatic conditions, temperature decreases due to thermo elastic effect. Beyond the yield point, a sudden reversal in the direction of temperature change occurs as thermal energy is released when plastic deformation occurs. Here, the irreversible work done on the material is converted

into heat resulting in increase in temperature Hence the elastic-plastic boundary (plastic zone) is the region, where the temperature rise is zero. Jordan et al. [11] obtained the plastic zone size ahead of crack tip by similar method. Typical plastic zone sizes of the specimens with cracks at various Stainless steel and HAZ of carbon steel are shown in Fig. 11. The plastic zones in CS are much higher than SS in view of the lower yield strength of CS.

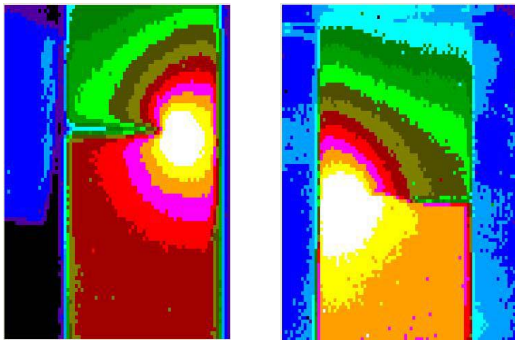

Fig. 11 IR Thermography images showing plastic zone sizes of (a) Stainless steel, (b) HAZ of carbon steel

The observation of different plastic zone sizes at the two material interfaces has an effect on the plasticity induced crack closure during fatigue crack growth. This would also alter the stress distribution ahead of the crack tip, thereby affecting the crack tip stress intensity factor.

V. Conclusion

The present study was carried out to characterize the FCG rate of dissimilar weldment of stainless steel and carbon steel using constant amplitude FCG test and Infrared Thermography technique. Based on this study the following can be inferred:

- The resistance to crack growth rate decreased with load ratio at all regions of the weldment, except in case of HAZ of carbon steel due to crack closure effect. HAZ of CS experience crack closure effect at large ΔK regions. This may be due to the non uniformity in the crystal structure caused by overheating during welding or roughness induced.
- Weld metal exhibited lower crack growth rate at intermediate ΔK region and CS region showed the highest rate.
- Fracture toughness of HAZ seems to be lower compared to the respective parent metals and K_{th} shows the reverse trend.
- IRT measurement suggest that the temperature response curve at the crack tip location exhibited three distinct regions
- Rise in the temperature at the crack tip correlated well with the fracture toughness values determined by constant amplitude fatigue crack growth test except in case of HAZ of CS.

References

[1] H. K. Lee, K. S. Kim, C. M. Kim, "Fracture Resistance of a Steel Weld Joint Under Fatigue Loading, Engineering Fracture mechanics", 2000.
[2] B. K. Choudhary, M. Roedig and S. L. Mannan, "Fatigue Crack Growth Behavior of Base Metal, Weld Metal and Heat Affected Zone of Alloy 800 at 823 K", 2004.
[3] S. J. Maddox, "Assessing the Significance of Flaws in Welds Subject to Fatigue", *Welding J.*, 1974.
[4] Laurent Cretegny, Ashok Saxena, "Fracture Toughness Behavior of Weldments with Mis-Matched Properties at Elevated Temperature"., Int. J. Fracture, Vol 92, No. 2, 1998.
[5] B. Bruzek, E. Leidich, "Evaluation of Crack Growth at Weld Interface between Bronze and Steel", *International Journal of Fatigue*, 2007.
[6] Zehnder AT, Rosakis Ares J., "Temperature Rise at the Tip of Dynamically Propagating Cracks: Measurements Using High-speed Infrared Detectors", *Experimental Techniques in Fracture*, 1993.
[7] Shockey DA, Kalthoff JF, Klemm W, Winkler S., "Simultaneous Measurement of Stress Intensity and Toughness for Fast Running Cracks in Steel", *Exp Mech* 1983.
[8] Montgomery DG, "The Temperature Wave Method of Determinating Fracture Toughness Values Due to Crack Propagation", *J Material Science* 1975.
[9] "T. Yamauchi, H. Hirano, Examination of Onset of Stable Crack Growth Under Fracture Toughness Testing of Paper", *Journal of Wood Science*, 2000.
[10] B.Yang, P.K. Liaw, M. Morrison, C.T. Liub, R.A. Buchanana, J.Y. Huangc,R.C. Kuo, J.G. Huang, and D.E. Fielden (2005), "Temperature evolution during fatigue damage", *Intermetallics* ,13, 419–428.
[11] Jordan Eric, H., "Notch-root plastic response by temperature measurement", *Exp. Mech*, 1985.